

Marginal Structural Modeling of Representative Treatment Trajectories

Jiewen Liu^{*1}, Todd A. Miano^{†1}, Stephen Griffiths^{‡2}, Michael G.S. Shashaty^{§2}, and Wei Yang^{¶1}

¹Department of Biostatistics, Epidemiology and Informatics, Perelman School of Medicine, University of Pennsylvania

²Pulmonary, Allergy, and Critical Care Division, Perelman School of Medicine, University of Pennsylvania

Abstract

Marginal structural models (MSMs) are widely used in observational studies to estimate the causal effect of time-varying treatments. Despite its popularity, limited attention has been paid to summarizing the treatment history in the outcome model, which proves particularly challenging when individuals' treatment trajectories exhibit complex patterns over time. Commonly used metrics such as the average treatment level fail to adequately capture the treatment history, hindering causal interpretation. For scenarios where treatment histories exhibit distinct temporal patterns, we develop a new approach to parameterize the outcome model. We apply latent growth curve analysis to identify representative treatment trajectories from the observed data and use the posterior probability of latent class membership to summarize the different treatment trajectories. We demonstrate its use in parameterizing the MSMs, which facilitates the interpretations of the results. We apply the method to analyze data from an existing cohort of lung transplant recipients to estimate the effect of Tacrolimus concentrations on the risk of incident chronic kidney disease.

1 Introduction

In observational studies involving treatments that may change over time, marginal structural models (MSMs) have been widely adopted by researchers as they provide consistent estimates of the causal effects by properly adjusting for

*jiewen.liu@pennmedicine.upenn.edu

†todd.miano@pennmedicine.upenn.edu

‡Stephen.Griffiths@Pennmedicine.upenn.edu

§shashatm@pennmedicine.upenn.edu

¶weiyang@pennmedicine.upenn.edu

time-dependent confounding using inverse probability weighting (IPW) (Robins, Hernan, & Brumback, 2000). To use MSMs for causal effect assessment, users need to specify (i) a propensity score model for the treatment of interest and (ii) an outcome model that explicitly parameterizes the causal association between the treatment history and outcome. Regarding (i), prior studies explored different weight choices to enhance the efficiency and stability of causal estimates in various settings (Hernán, Brumback, & Robins, 2000; Cole & Hernán, 2004; McCaffrey, Lockwood, & Setodji, 2013; Lee, Lessler, & Stuart, 2011). However, for (ii), there is limited research in parameterizing the outcome model in the complex time-varying treatment setting, which often hinders the interpretation of the causal estimates.

Since there is often a large number of unique treatment regimes in studying time-varying treatments, it is impractical to account for all potential treatment combinations in modeling the outcome. For instance, in a clinical study spanning a week where each patient receives a daily binary treatment, a model with over $2^7 = 128$ parameters becomes unfeasible to evaluate. As a result, in practice, researchers often resort to practical metrics for time-varying treatments such as averages, maximums and minimums (Wang et al., 2010; Jimenez et al., 2021). For treatment histories with complex patterns over time, these metrics may be over-simplified and thus fail to address the clinical question of interest. There have been some works of history-adjusted MSMs (Joffe, Santanna, & Feldman, 2001; Petersen, Deeks, Martin, & Van Der Laan, 2007), which can be utilized to reduce model complexity by restricting the time window of treatment of interest and obtain interpretable results; Platt, Brookhart, Cole, Westreich, and Schisterman (2013) also studied the functional form of the metrics choices and the goodness of MSM fit via the information criterion. Nonetheless, the challenge persists when the interest lies in the causal effect of the whole treatment history on the outcome.

This common challenge is also confronted when analyzing data from a prospective cohort of lung transplant recipients. Enrolled patients gave informed consent to participate in the Lung Transplant Outcomes Group (LTOG) study, a multicenter prospective cohort designed to investigate the acute and long-term complications following lung transplantation (Farrell et al., 2022). We consider LTOG participants enrolled at the Hospital of the University of Pennsylvania (Penn) from 2005-2015 to evaluate the effect of Tacrolimus (TAC) concentration within 7 days after lung transplantation on the long-term development of chronic kidney disease (CKD). TAC is a cornerstone immunosuppressive medication prescribed to > 90% of lung transplant recipients that have known acute and chronic nephrotoxic effects. Yet, the impact of perioperative TAC concentrations on CKD risk is unknown. Under the current clinical practice, physicians typically initiate TAC dosing on Day 1 with a conservative dosage, targeting a low TAC concentration in patients' blood, with slight modifications based on baseline covariates such as age and BMI. Clinical teams made adjustments to the dosage, as needed, depending on daily measured TAC blood concentrations (with a typical target of 8 – 12ng/ml), use of potentially interacting medications, postoperative physiologic derangements that may impact drug metabolism, and the development or perceived risk of TAC adverse effects. In particular, the development of acute kidney injury (AKI), a sudden loss in kidney function and known side effects of TAC, are important drivers of clinicians' perioperative TAC dosing decisions and targets (Farrell et al., 2022). Consequently, TAC concentrations exhibit noticeable variations

with different dosing intensities and drug metabolism for each patient from Day 2 to Day 7.

Tackling this challenge can be seen as parameterizing an outcome model under the MSM framework that is simultaneously feasible and offers a causal interpretation of practical relevance to scientific questions. Latent growth curve (LGC) analysis has been used to detect latent classes that explain observed changes and to model class-specific trajectories for each individual. In Penn LTOG participants, the observed variations in 7-day TAC concentrations also show the potential to be characterized by a few representative trajectory functions. This inspires the application of LGC models to summarize the trajectories of TAC concentrations through latent class membership, which can then be used to parameterize the outcome model.

In this paper, we conceptualize each individual's treatment history as a measurement of a few underlying representative trajectories to which they adhere. We use LGC analysis to identify these representative trajectories and each individual's probability of belonging to these latent trajectories. We use the posterior probabilities to represent each individual trajectory and demonstrate how they can be modeled to provide new causal interpretations on the trajectory level. In the Discussion section, we explore the more fundamental ideas behind the proposed approach, compare it with other practices in parameterizing the outcome model, and examine its potential applications in other observational studies.

The paper is organized as follows: Section 2 begins with a review of the Penn dataset, serving as a motivating example. We introduce the standard MSM setup and elaborate on the challenge of parameterizing the outcome model. Subsequently, we present a new approach using LGC analysis to summarize the treatment histories and develop a causal model with clinically meaningful interpretations. In Section 3, we present details of analyzing the dataset from the Penn dataset with the proposed approach. Section 4 concludes with a discussion.

2 Methodology

2.1 Dataset, Notation and Causal Structure

In the study, we are interested in the effect of TAC concentrations within the first seven days after lung transplantation on the long-term risk of CKD. We excluded subjects who met the definition of CKD within the first seven days following the lung transplantation as they are not of clinical interest. Consequently, we included 363 individuals in the analysis. The relationship between the treatment, covariate and outcome of interest can be represented by the DAG in Figure 2, assuming there is no unmeasured confounder U in the graph. A main characteristic of the DAG is that no patient information (including both treatment and other covariates) is considered after the 7-day period and until the occurrence of CKD or end of study follow-up, which is one year after lung transplantation. It is a form of partial exposure, which was studied in previous literature (Vansteelandt, Mertens, Suetens, & Goetghebeur, 2009).

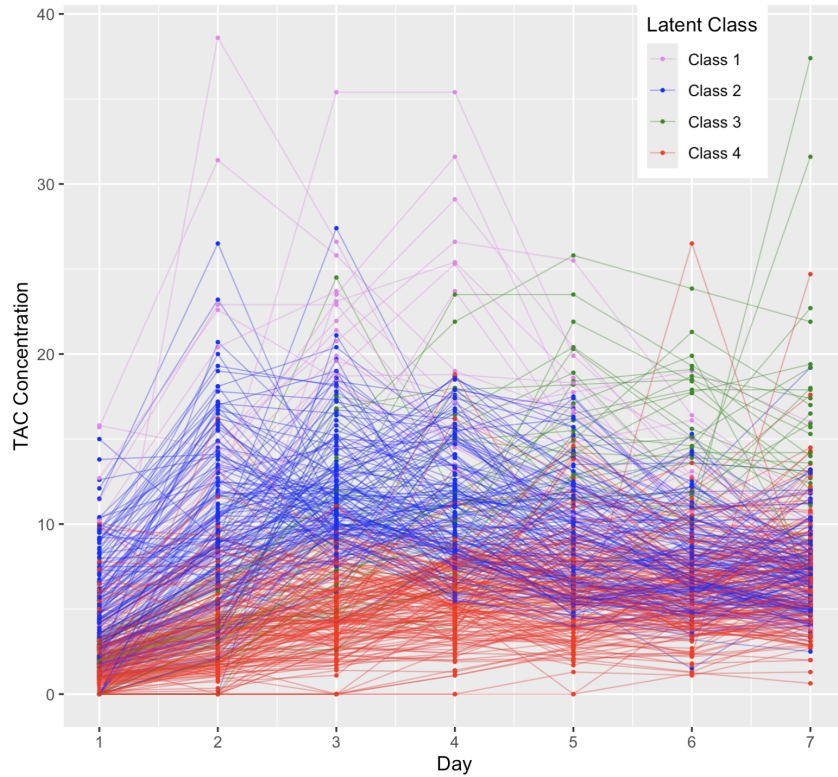


Figure 1: Curve plot of 7-day TAC concentrations for each patient with their latent class membership distinguished by the color.

With the above notations, we proceed to the potential outcome framework (Rubin, 1974). We use $\bar{A}_k = (A_1, \dots, A_k)$ and $\bar{L}_k = (L_1, \dots, L_k)$ to denote the history of treatment and covariates up to day k , respectively. $T^{\bar{a}^k}$ denotes a subject's potential survival time had they, possibly contrary to fact, received treatment $\bar{A}_k = \bar{a}_k$. We make three standard assumptions:

(i) Consistency:

$$T = T^{\bar{a}^k} \text{ if } \bar{A}_k = \bar{a}_k.$$

(ii) Sequential Ignorability:

$$T^{\bar{a}^{k-1}, a_k} \perp A_k | \bar{A}_{k-1} = \bar{a}_{k-1}, \bar{L}_k$$

(iii) Positivity:

$$f_{A_k | \bar{A}_{k-1}, \bar{L}_k}(a_k | \bar{a}_{k-1}, \bar{l}_k) > 0 \text{ if } f_{\bar{A}_{k-1}, \bar{L}_k}(\bar{a}_{k-1}, \bar{l}_k) \neq 0, \text{ for all possible } (\bar{a}_{k-1}, \bar{l}_k).$$

Under these three assumptions, the parameters in the MSMs can be identified from the observed data. Implications of these assumptions has been discussed in previous literature, e.g., Cole and Hernán (2008).

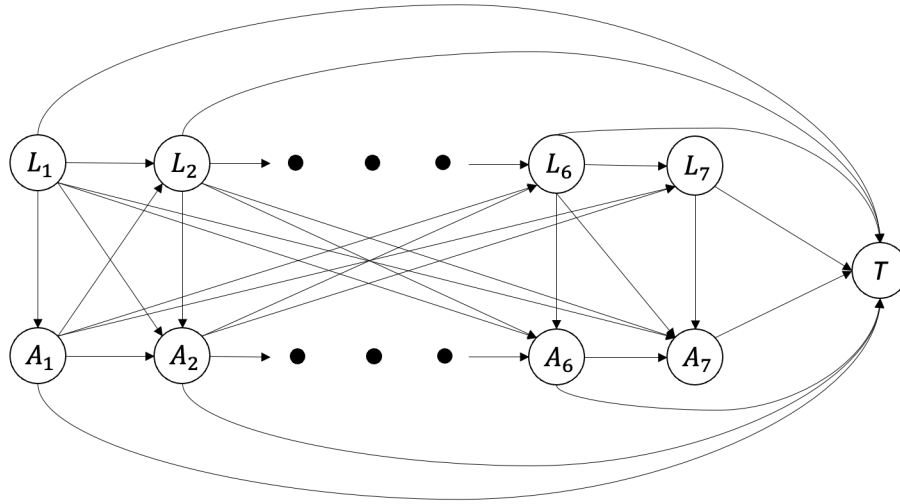


Figure 2: The DAG for the 7-day TAC concentration. A_t denotes the TAC concentration. L_t denotes measured covariates. T denotes the event time of CKD diagnosis.

2.2 Marginal Structural Models

Marginally structural models constitute a class of statistical models for estimating marginal causal effects of time-varying treatments (Robins et al., 2000). MSM analysis requires a propensity score model for the probability of the treatment assignment at each time point and an outcome model parameterizing the causal relationship between the treatment history and potential outcomes. These causal effects are identified under the assumptions outlined in Section 2.1, and IPW estimators are constructed to consistently estimate the causal parameters in the outcome model. A general MSM model for the functional of potential outcome $\eta(T^{\bar{a}_k})$ with the treatment history \bar{a}_k to day k and baseline covariates V is represented as

$$\eta(T^{\bar{a}_k}) = q(\bar{A}_k = \bar{a}_k, V).$$

Returning to the Penn lung transplant dataset, researchers are interested in the causal effect of 7-day TAC concentrations on the development of CKD. We adopt the marginal structural Cox proportional hazards (MSM-Cox) model to establish the causal relationship between 7-day TAC concentrations \bar{A}_7 and the potential survival outcome of CKD diagnosis time $T^{\bar{a}_7}$ with the adjustment of baseline covariates V . The model without interactions between \bar{A}_7 and V is represented as

$$\lambda_{T^{\bar{a}_7}}(t|V) = \lambda_0(t) \exp\{q_1(\bar{A}_7) + q_2(V)\}, \quad (1)$$

where λ_0 denotes the baseline hazard, and q_1 and q_2 are user-specified functions with inputs \bar{A}_7 and V , respectively. The selection of q_1 is contingent upon the scientific questions to be addressed. Properly specifying q_1 is pivotal in

answering these questions as it directly links to the interpretation of the result. Within model (1), the causal contrast of interest can be formally defined as the hazard ratio of potential outcomes under two different 7-day TAC concentration regimes \bar{a}_7 and \bar{a}'_7 :

$$\frac{\lambda_{T\bar{a}_7}(t|V)}{\lambda_{T\bar{a}'_7}(t|V)} = \exp\{q_1(\bar{a}_7) - q_1(\bar{a}'_7)\}.$$

A common challenge faced by researchers is that, given the limited sample size, exhaustive exploration of the sample spaces of treatment combinations, which is \mathbf{R}^7 or 2^7 (dichotomized version) for 7-day TAC concentrations, is not feasible in the outcome model. Consequently, researchers often turn to rudimentary metrics like the mean of the treatment history as a pragmatic solution. For example, a structural model using 7-day average TAC concentration is as follows

$$\lambda_{T\bar{a}_7}(t|V) = \lambda_0(t) \exp\{\beta_a \cdot \text{mean}(\bar{A}_7) + \beta_v^T V\}$$

As highlighted earlier, these metrics may be too simplified to adequately summarize treatment histories to provide meaningful guidance for clinical practices. Inspired by distinct patterns observed from 7-day TAC concentrations, we propose a new approach for specifying q_1 in the following sections.

The next step in constructing the IPW estimator is weight estimation. There are various choices for weights and their estimation methods. We choose the commonly used stabilized weight:

$$sw = \prod_{k=1}^7 \frac{P(A_k = a_k | \bar{A}_{k-1}, V)}{P(A_k = a_k | \bar{A}_{k-1}, \bar{L}_k, V)}.$$

Details on estimating the stabilized weights for 7-day TAC concentrations are provided in Section 3. The stabilized weight is the cumulative product from Day 1 to Day 7 as the exposure of interest is only up to 7 days after lung transplantation. As we have discussed in Section 2.1, this partial exposure simplifies both the weight calculation and the MSM-Cox model specification.

2.3 Characterizing Treatment Trajectories Through Latent Growth Curve Analysis

Latent Growth Curve (LGC) analysis is a statistical technique for examining longitudinal data patterns (Duncan & Duncan, 2004). The LGC model assumes that each subject is associated with a latent class membership $M = c \in \{1, \dots, C\}$. Within each class c , individuals follow a class-specific growth curve, also termed trajectory.

In the LTOG study, inspired by temporal patterns of TAC concentrations, we conceptualize the observed treatment

history curves can be represented by a few latent trajectories. We use LGC modeling to identify these latent treatment trajectories. Specifically, we model the 7-day TAC concentration A_t as a mixture of Gaussian growth curves parameterized by a function of the day after lung transplantation $\psi(D_t; \alpha^{(c)})$ with class-specific parameters $\alpha^{(c)}$ and an independently distributed normal error term, ϵ_t . Given latent class membership $M_i = c$,

$$A_{it} = \psi(D_{it}; \alpha^{(c)}) + \epsilon_{it} \quad (2)$$

where $D_{it} = t, \epsilon_{it} \stackrel{i.i.d.}{\sim} N(0, \sigma^2)$, for $i = 1, \dots, n, t = 1, \dots, 7, c \in \{1, \dots, C\}$. Figure 3 gives a graphical illustration of the data generation mechanism under the LGC model, in which the function ψ takes a quadratic function of the day D_t with class-specific coefficients $\alpha^{(c)} = (\alpha_0^{(c)}, \alpha_1^{(c)}, \alpha_2^{(c)})$. More sophisticated LGC models with different implementations are also available, including adjustments for baseline covariates, the application of link functions, and the incorporation of random effects for model parameters (Preacher, 2008). For our purpose, we proceed with the fixed effect LGC model with the day since lung transplantation as the only covariate.

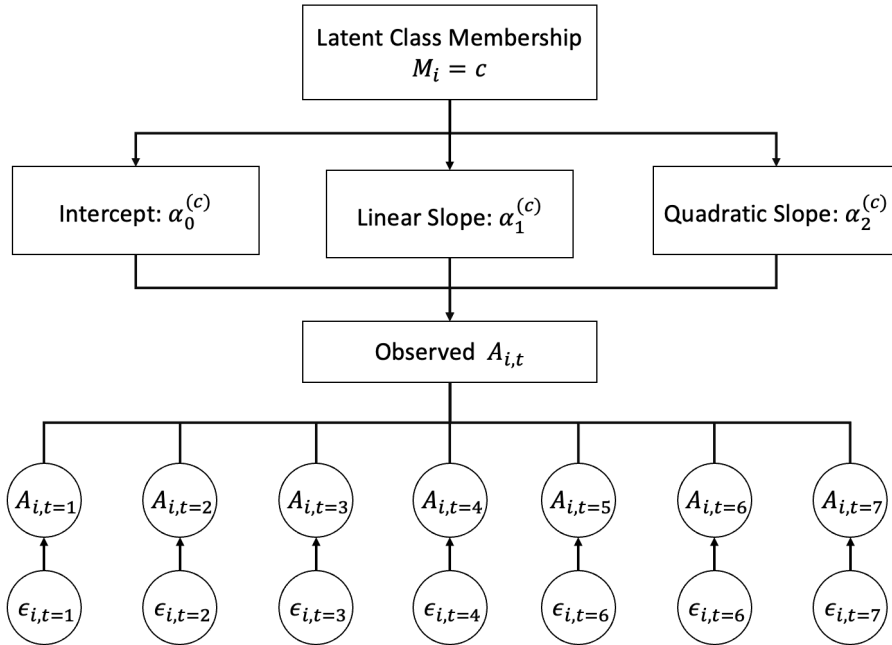


Figure 3: A graphical representation of the data generation mechanism under the LGC model with quadratic terms for time-varying covariates and observations across 7-time points for i -th subject with latent class membership $M_i = c$

In the Penn lung transplant cohort, for all patients, given observed 7-day TAC concentrations $\mathbf{A} = (\bar{A}_{17}, \dots, \bar{A}_{n7})$ and days $\mathbf{D} = (\bar{D}_{17}, \dots, \bar{D}_{n7})$ and latent class memberships $\mathbf{M} = (M_1, \dots, M_n)$, model (2) has the likelihood function with parameters $(\alpha, \sigma^2, \theta)$, where $\alpha = (\alpha^{(1)}, \dots, \alpha^{(C)})$ and $\theta = (\theta_1, \dots, \theta_C)$:

$$M_i \sim \text{Multinomial}(\theta), A_{it}|D_{it}, M_i \sim N(\psi(D_{it}; \alpha^{(M_i)}), \sigma^2);$$

$$\begin{aligned}
& f(\mathbf{A}, \mathbf{M} | \mathbf{D}, \alpha, \sigma^2, \theta) \\
&= f(\mathbf{A} | \mathbf{M}, \mathbf{D}, \alpha, \sigma^2) f(\mathbf{M} | \theta) \\
&= \prod_{i=1}^n \left(\prod_{j=1}^C \prod_{t=1}^7 \frac{1}{\sqrt{2\pi\sigma^2}} \exp \left\{ -\frac{1}{2\sigma^2} (A_{it} - \psi(D_{it}; \alpha^{(j)}))^2 \right\} \theta_j \right)^{I(M_i=j)}.
\end{aligned}$$

Several established methods, including the Expectation-Maximization (EM) algorithm (Muthén & Shedden, 1999), can be used to evaluate the above likelihood function involving the latent variable \mathbf{M} (Ng, Carpenter, Goldstein, & Rasbash, 2006). By evaluating this likelihood function, we can obtain the estimated $(\hat{\alpha}, \hat{\sigma}^2, \hat{\theta})$ and posterior probabilities of latent class membership for any subject with given treatment history (\bar{A}_7, \bar{D}_7) :

$$\Pr(M = c | \bar{A}_7) = \Pr(M = c | \bar{A}_7, \bar{D}_7, \hat{\alpha}, \hat{\sigma}^2, \hat{\theta}) = \frac{f(\bar{A}_7, \bar{D}_7, M = c | \hat{\alpha}, \hat{\sigma}^2, \hat{\theta})}{\sum_{j=1}^C f(\bar{A}_7, \bar{D}_7, M = j | \hat{\alpha}, \hat{\sigma}^2, \hat{\theta})}, \quad c \in \{1, \dots, C\}.$$

To clarify, we write $\Pr(M = c | \bar{A}_7)$ instead of $\Pr(M = c | \bar{A}_7, \bar{D}_7)$ because day $\bar{D}_7 = (1, 2, 3, 4, 5, 6, 7)$ is fixed for all patients in the Penn lung transplant cohort.

For each subject, we use the posterior probabilities of belonging to each latent class $p = (p_1, \dots, p_C)^T$ as a summary of treatment trajectory, where $p_c = \Pr(M = c | \bar{A}_7)$ and $\sum_{j=1}^C p_j = 1$. In the LTOG study, the posterior probability vector p characterizes the similarity between an individual patient's 7-day TAC concentration trajectory and representative trajectories $(1, \dots, C)$ identified from the overall patient population. For subsequent analysis, we can either follow the principle of hard-thresholding, that is, assigning each patient to the class c with the highest posterior probability p_c , or the principle of soft-thresholding, using the probability vector p as a holistic characterization of the patient's treatment trajectory without explicitly assigning each patient to a specific class.

2.4 Outcome Model Specification

The previous section has introduced a perspective on viewing each individual treatment history as adherence to representative treatment trajectories identified by the LGC, where the posterior probability serves as a measure for the degree of adherence. Next, we demonstrate how we use a subject's latent class membership to specify the outcome model within the MSM framework. In the LTOG study, the outcome models can be parameterized as follows:

$$\lambda_{T^{a_7}}(t | V) = \lambda_0(t) \exp \left\{ \sum_{j=1}^{C-1} \beta_j I(p_j = \max\{p\}) + q_2(V) \right\}.$$

We are interested in causal parameters β_j for $j \in 1, \dots, C-1$, and class C is set as the reference class and so $(C-1)$ coefficients are estimated. Alternatively, we can use the posterior probabilities directly in the MSM outcome model

$$\lambda_{T\bar{a}_T}(t|V) = \lambda_0(t) \exp\left\{\sum_{j=1}^{C-1} \beta_j p_j + q_2(V)\right\}.$$

In both models, $\exp\{\beta_c\}$ can be interpreted as the survival benefit on the hazard rate scale if the patient follows class c 's treatment trajectory compared to the reference class C . In the context of TAC concentrations, each element p_c in the posterior probability vector p corresponds to an identified representative treatment trajectory, through which the Cox model is parameterized to compare the hazard rates between different representative trajectories.

To construct IPW estimators for the above outcome models, we can follow the same routine of weight computation as discussed in Section 2.2. This is because the purpose of weighting is to achieve treatment ignorability in the weighted population. Hence, any function of the treatment history, including the proposed adherence metric, also satisfies the ignorability condition after weighting.

3 Application: Effect of TAC Concentration on Risk of CKD

We applied the proposed method to analyze the data collected from Penn. The goal is to assess the causal association between TAC concentrations within 7-days after lung transplantation and the time to incident CKD during the first post-transplant year. Table 1 presents a few key patient characteristics. Using R package `lcmm` (Proust-Lima, Philipps, &

Variable	Overall
Sample Size – n	362
Age of Recipient (mean (SD))	56.92 (10.23)
Race (%)	
White	317 (87.6)
African American	(8.8)
Other	13 (3.6)
Female (%)	151 (41.6)
BMI kg/m^2 (mean (SD))	26.42 (5.18)
Preoperative Serum Creatinine, mg/dL (mean (SD))	0.89 (0.28)

Table 1: Overall patient characteristics.

Liquet, 2017; Proust-Lima, Philipps, Diakite, & Liquet, 2023), we first build an LGC model for 7-day TAC concentrations to identify representative treatment trajectories and latent class membership for each patient. After examining the p -values of class-specific coefficients and higher-order terms, we find the following model with the quadratic function of

the predictor day with 4 latent classes fits our data the best. Given the latent class membership $M_i = c$:

$$A_{it} = \alpha_0^{(c)} + \alpha_1^{(c)} D_{it} + \alpha_2^{(c)} D_{it}^2 + \epsilon_{it}, \quad (3)$$

where $\epsilon_{it} \stackrel{i.i.d}{\sim} N(0, \sigma^2)$ for $i = 1, \dots, n$, $t = 1, \dots, 7$, $c \in \{1, \dots, 4\}$. We assigned each patient to the class with the highest probability estimated by the LGC model. Table 2 presents the number of patients and survival outcomes in each latent class. Figure 4 gives a closer look into each latent class. The left graph of Figure 4 visualizes the 4 class-specific trajectories differentiated by the LGC model (3). The right graph of Figure 4 plots curves of each class's patients' 7-day TAC concentrations. We see patients' TAC concentrations in each latent class exhibit different patterns and align well with corresponding class-specific trajectories visualized in the left graph of Figure 4. This alignment indicates a good fit of our tailored model (3), effectively identifying representative treatment trajectories in this patient population. Additionally, over 80% of patients have the posterior probability of belonging to a certain latent class exceeding 0.8.

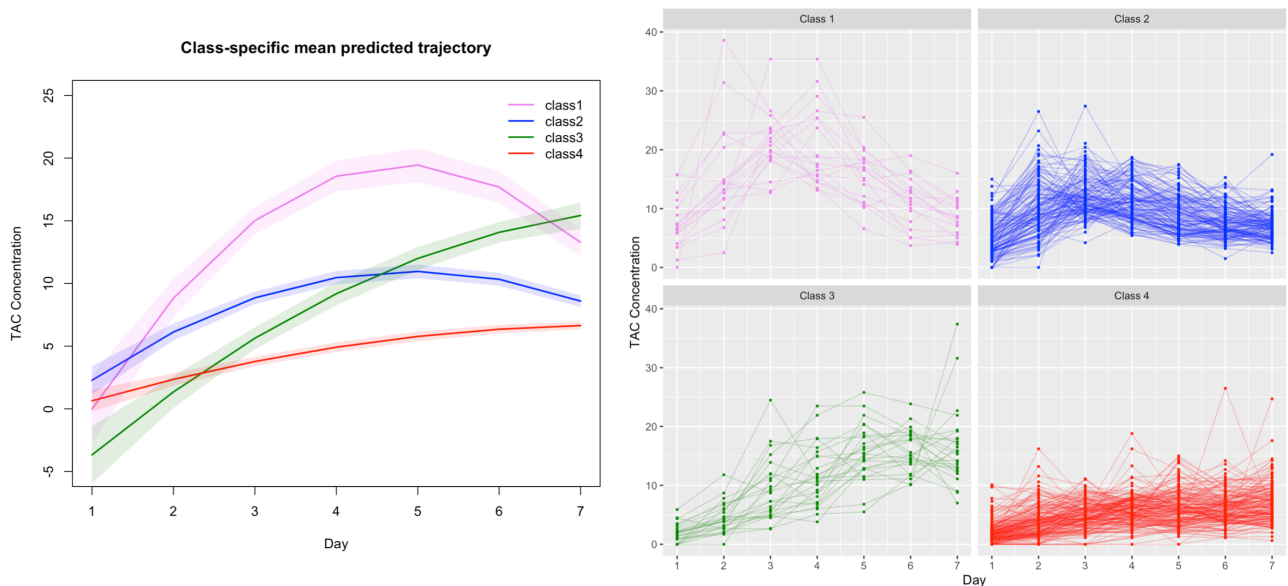


Figure 4: The visualization of the fitted LGC model. The left graph displays 4 treatment trajectories as well as their 95% confidence intervals (shaded regions) corresponding to different latent classes. The right graph plots curves for patients' 7-day TAC concentrations in each latent class.

Variable	Class 1	Class 2	Class 3	Class 4
Sample Size	19	141	26	176
CKD Occurrence (%)	1 (5.3)	74 (52.5)	15 (57.7)	93 (52.8)
CKD Event Rate (%)	0.448	0.616	1.2	0.670
Death (%)	8 (42.1)	19 (13.5)	13 (50.0)	34 (19.3)
Death without CKD Occurrence (%)	8 (42.1)	9 (6.4)	9 (34.6)	21 (11.9)

Table 2: Patient's survival outcome by the latent class.

For the weight estimation, we divided daily TAC concentration into 4 categories based on quartiles and build two paral-

lel multinomial logistic regression models to estimate the numerator and denominator respectively in the formula for stabilized weight calculation. The model includes treatment and covariate history up to prior two days. For the numerator, the model is conditional on the past two-day TAC concentrations and baseline covariates. For the denominator, the model is additionally conditional on the past two-day time-dependent covariate history. The baseline covariates and the time-varying covariates on day 0 given in Table 3 are included in both the numerator and the denominator models.

	Variable Included
Baseline Covariates	age, race, gender, BMI, preoperative serum creatinine level, pgd3, iTot, diag2, procType2, cr_base, cpbCat, crystalEver, induction.
Time-Varying Covariates	aki, chl_Int2, pltInt2, hctInt2, steroids2, amio2, loopCat2, vanco2, viral2, gramNeg2, gramPos2, press2, and prolif2.

Table 3: Variables included in propensity score models.

Finally, using the posterior probability of latent class membership, we fit two Cox proportional hazards models in the weighted population, where Class 4 is set as the reference category:

by hard-thresholding:

$$\lambda_{T_i^{\hat{a}_7}}(t|V) = \lambda_0(t) \exp\left\{\sum_{j=1}^3 \beta_j I(p_{ij} = \max\{p_i\}) + \beta_v^T V\right\};$$

by soft-thresholding:

$$\lambda_{T_i^{\hat{a}_7}}(t|V) = \lambda_0(t) \exp\left\{\sum_{j=1}^3 \beta_j p_{ij} + \beta_v^T V\right\}.$$

The estimated model coefficients are presented in Table 3. In the model with class membership as the predictor, the risk of developing CKD among those in class 3 is 2.60 times higher compared to the reference class 4 ($HR = \exp\{\beta_3\} = \exp\{0.956\} \approx 2.60$, 95% CI: [1.22, 5.54]). The risks of CKD for class 1 and 2 are not significantly different from the reference class 4. The results from the Cox regression with the posterior probability of class membership were similar.

Class Membership as Predictor				Posterior Probability of Class Membership as Predictor			
Term	Coefficient	Robust S.E.	P-Value	Term	Coefficient	Robust S.E.	P-Value
Class 1 - β_1	-0.711	0.458	0.120	Class 1 - β_1	-0.669	0.456	0.143
Class 2 - β_2	0.068	0.213	0.751	Class 2 - β_2	-0.063	0.245	0.795
Class 3 - β_3	0.956	0.386	0.013	Class 3 - β_3	1.012	0.397	0.011

Table 4: Coefficients of two fitted Cox models with different predictors. (Class 4 is set to the reference class.)

4 Discussion

In this paper, we developed an approach to address the challenge of parameterizing the outcome model in MSM modeling when treatment regimes exhibit distinct temporal patterns. We used latent growth curve analysis to identify representative treatment trajectories and the estimated posterior probabilities of class membership to characterize each individual treatment trajectory. We demonstrated how this metric can be utilized to construct simple outcome models and provided straightforward interpretations in analyzing data from the Penn lung transplant cohort.

LGC modeling is used as a dimension reduction tool to characterize the extremely large number of possible treatment regimes, using either a fixed class membership or a vector of posterior probabilities of belonging to each identified latent class. In the hard-threshold approach, each individual treatment trajectory is assigned to one of a few latent classes. The average treatment trajectory within each latent class is a representation of the treatment regimes experienced by those within that class. In the structural model, instead of using each individual treatment regime, we modeled the outcome as a function of the latent class membership. The parameter associated with each latent class indicator in the outcome model corresponds to the comparison of outcomes with the reference class. It can be interpreted as a causal comparison of what would happen if all individuals in the study population had followed the class-specific representative treatment trajectory versus the reference class. In the soft-threshold approach, instead of assigning each individual to a fixed class membership, the posterior probability from the LGC analysis is used to represent how close each individual treatment trajectory is to the cluster average treatment experience. Similar to the idea of compliance score, the posterior probability vector can also be viewed as a compliance measure of each individual treatment regime with respect to the representative treatment trajectories for the different latent classes. This view seems easier to be adopted and understood. In the outcome model, we include the posterior probabilities for each latent class instead of the assigned class membership. The coefficient for each posterior probability for a specific latent class has the same interpretation as the model using the assigned class membership. It can be interpreted as a causal comparison of what would happen if all individuals in the study population were fully compliant with a class-specific representative treatment regime versus the reference class.

In addition to the comparison of representative treatment regimes, we can also estimate the effect associated with an arbitrary treatment regime, using either the hard-threshold or soft-threshold approach. An arbitrary treatment regime can be approximated by a linear combination of the representative treatment trajectories for the different latent classes. A linear combination of the causal parameters in the outcome model using the same set of coefficients is an estimate of the causal contrast of what would happen if all individuals had followed this particular arbitrary treatment regime versus the representative treatment regime for the reference class. Similar ideas were proposed elsewhere in the literature (Anderson et al., 2015).

Depending on the study objective, alternative methods can be used to summarize diverse treatment regimes to facilitate the outcome model specification. For example, Joffe, Yang, Brunelli, and Feldman (2007) studied the causal association of hemoglobin variability on mortality in hemodialysis patients. They fit a linear function of hemoglobin on time within each individual and used the intercept, slope and residual standard deviation from the linear regression to characterize hemoglobin trajectories over time.

We applied the proposed method and identified a few representative treatment trajectories in the Penn lung transplant cohort. We also found that a more aggressive increase of Tacrolimus concentration within 7 days after lung transplantation is associated with an increased risk of chronic kidney disease compared to a more conservative treatment regime. Additional work may be needed to determine if these trajectories are robust and generalizable using more contemporary transplant data from multiple clinical centers. Additionally, efforts should focus on understanding how accurately these latent classes reflect practices in relation to patient- and time-specific drug metabolism, with the ultimate goal of developing better clinical practices to maximize patient benefits.

References

- Anderson, A. H., Yang, W., Townsend, R. R., Pan, Q., Chertow, G. M., Kusek, J. W., . . . others (2015). Time-updated systolic blood pressure and the progression of chronic kidney disease: a cohort study. *Annals of internal medicine*, 162(4), 258–265.
- Cole, S. R., & Hernán, M. A. (2004). Adjusted survival curves with inverse probability weights. *Computer methods and programs in biomedicine*, 75(1), 45–49.
- Cole, S. R., & Hernán, M. A. (2008). Constructing inverse probability weights for marginal structural models. *American journal of epidemiology*, 168(6), 656–664.
- Duncan, T. E., & Duncan, S. C. (2004). An introduction to latent growth curve modeling. *Behavior therapy*, 35(2), 333–363.
- Farrell, C., Miano, T. A., Griffiths, S., Christie, J. D., Diamond, J. M., & Shashaty, M. G. (2022). Early post-lung transplant calcineurin inhibitor management varies widely: An international survey. *Clinical transplantation*, 36(2), e14510.
- Hernán, M. Á., Brumback, B., & Robins, J. M. (2000). *Marginal structural models to estimate the causal effect of zidovudine on the survival of hiv-positive men* (Vol. 11) (No. 5). LWW.
- Jimenez, M. P., Aris, I. M., Rifas-Shiman, S., Young, J., Tiemeier, H., Hivert, M.-E., . . . James, P. (2021). Early life exposure to greenness and executive function and behavior: an application of inverse probability weighting of marginal

- structural models. *Environmental Pollution*, 291, 118208.
- Joffe, M., Santanna, J., & Feldman, H. (2001). Partially marginal structural models for causal inference. In *American journal of epidemiology* (Vol. 153, pp. S261–S261).
- Joffe, M., Yang, W., Brunelli, S., & Feldman, H. (2007). Methodological issues in the study of the effects of hemoglobin variability.
- Lee, B. K., Lessler, J., & Stuart, E. A. (2011). Weight trimming and propensity score weighting. *PloS one*, 6(3), e18174.
- McCaffrey, D. F., Lockwood, J., & Setodji, C. M. (2013). Inverse probability weighting with error-prone covariates. *Biometrika*, 100(3), 671–680.
- Muthén, B., & Shedden, K. (1999). Finite mixture modeling with mixture outcomes using the em algorithm. *Biometrics*, 55(2), 463–469.
- Ng, E. S., Carpenter, J. R., Goldstein, H., & Rasbash, J. (2006). Estimation in generalised linear mixed models with binary outcomes by simulated maximum likelihood. *Statistical Modelling*, 6(1), 23–42.
- Petersen, M. L., Deeks, S. G., Martin, J. N., & Van Der Laan, M. J. (2007). History-adjusted marginal structural models for estimating time-varying effect modification. *American Journal of Epidemiology*, 166(9), 985–993.
- Platt, R. W., Brookhart, M. A., Cole, S. R., Westreich, D., & Schisterman, E. F. (2013). An information criterion for marginal structural models. *Statistics in medicine*, 32(8), 1383–1393.
- Preacher, K. J. (2008). *Latent growth curve modeling* (No. 157). Sage.
- Proust-Lima, C., Philipps, V., Diakite, A., & Liqueur, B. (2023). lcmm: Extended mixed models using latent classes and latent processes [Computer software manual]. Retrieved from <https://cran.r-project.org/package=lcmm> (R package version: 2.1.0)
- Proust-Lima, C., Philipps, V., & Liqueur, B. (2017). Estimation of extended mixed models using latent classes and latent processes: The R package lcmm. *Journal of Statistical Software*, 78(2), 1–56. doi: 10.18637/jss.v078.i02
- Robins, J. M., Hernan, M. A., & Brumback, B. (2000). *Marginal structural models and causal inference in epidemiology* (Vol. 11) (No. 5). Lww.
- Rubin, D. B. (1974). Estimating causal effects of treatments in randomized and nonrandomized studies. *Journal of educational Psychology*, 66(5), 688.
- Vansteelandt, S., Mertens, K., Suetens, C., & Goetghebeur, E. (2009). Marginal structural models for partial exposure regimes. *Biostatistics*, 10(1), 46–59.
- Wang, O., Kilpatrick, R. D., Critchlow, C. W., Ling, X., Bradbury, B. D., Gilbertson, D. T., . . . Acquavella, J. F. (2010). Relationship between epoetin alfa dose and mortality: findings from a marginal structural model. *Clinical Journal of the American Society of Nephrology*, 5(2), 182–188.